Results from the CALET Ultra-Heavy Cosmic-Ray Analysis

Wolfgang V. Zober, Brian F. Rauch, Nick Cannady, Yosui Akaike

for the CALET Collaboration

ICRC 2025

The Calorimetric Electron Telescope

- CALET launched to the ISS in August 2015 to determine the spectra of the electron-flux up to TeV energies.
  - While CALET was designed for electrons and possesses a normal incidence depth of 30 radiation lengths, it also has the dynamic range that’s capable of measuring elemental charge up to Z=40.
- The instrument consists of two layers of segmented plastic scintillators for the cosmic-ray charge identification (CHD), a 3 radiation length thick tungsten-scintillating fiber imaging calorimeter (IMC) and a 27 radiation length thick lead-tungstate calorimeter (TASC).
- Its main calorimeter is designed to measure the spectra of high energy cosmic-ray electrons, but has also made excellent measurements of cosmic-ray (CR) nuclei and gamma rays.

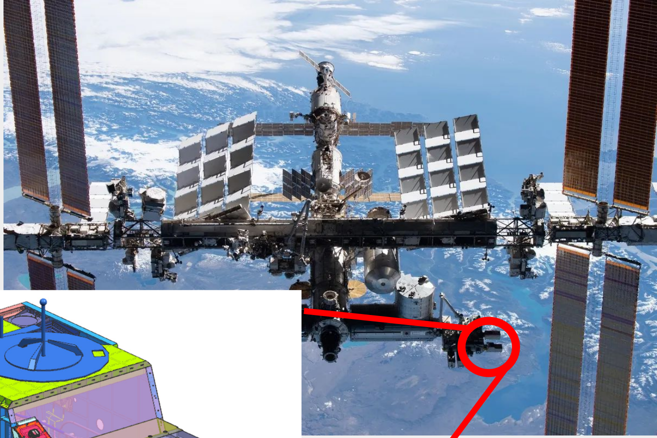

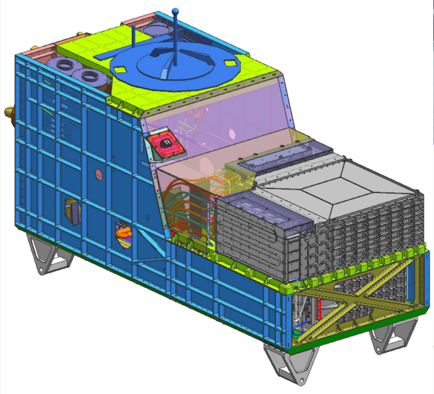

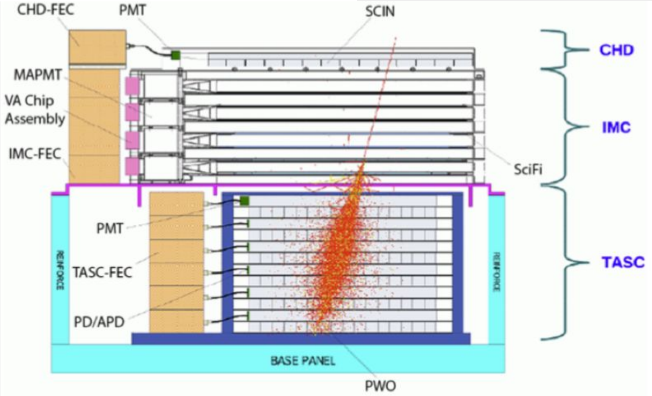

Ultra-Heavy Cosmic Ray Science

- Ultra-heavy cosmic rays (UHCR) provide clues into the source of all other cosmic rays: their acceleration mechanism, nucleosynthetic processes, etc.
- Provide insight into understanding the limits of the most energetic processes in our galaxy supernova, binary neutron star mergers

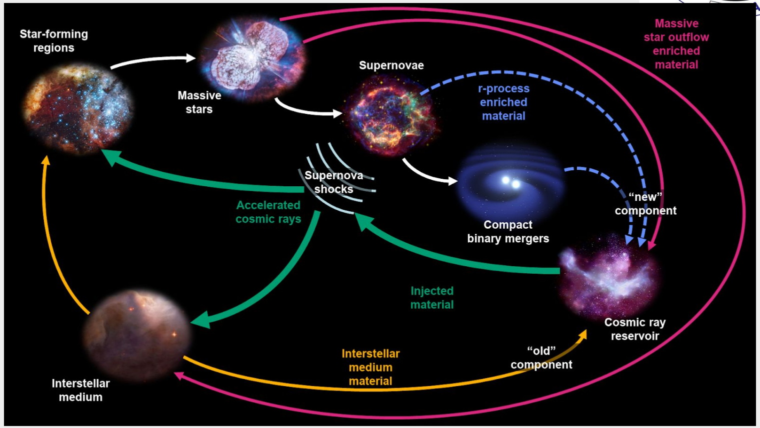

- Instruments that can do UHCR measurements for 30 ≤ Z ≤ 40 with single element resolution:
  - CALET on ISS within earth's magnetosphere with energy range, E > 1 GeV/nucleon
  - SuperTIGER which measures at similar energies to CALET.
    - Note, that as a stratospheric balloon payload, it has different systematics that include requiring atmospheric corrections.
  - ACE-CRIS at the L1 Lagrange point outside Earth's magnetosphere and an energy range ~100 – 500 MeV/nucleon.

Analysis of UH events

- This analysis uses 8 years of CALET UH-trigger data from 10/2015 through 11/2023.
- We add a constraint to the analysis that events pass through the top of the TASC. (~75 million events)
- This reduces statistics but the energy information allows for an improved charge assignment.
  - Allowing us to trade statistics for better resolution.
- We apply a number of secondary corrections over time bins and position in CHD, and perform charge assignment based on bins of deposited energy

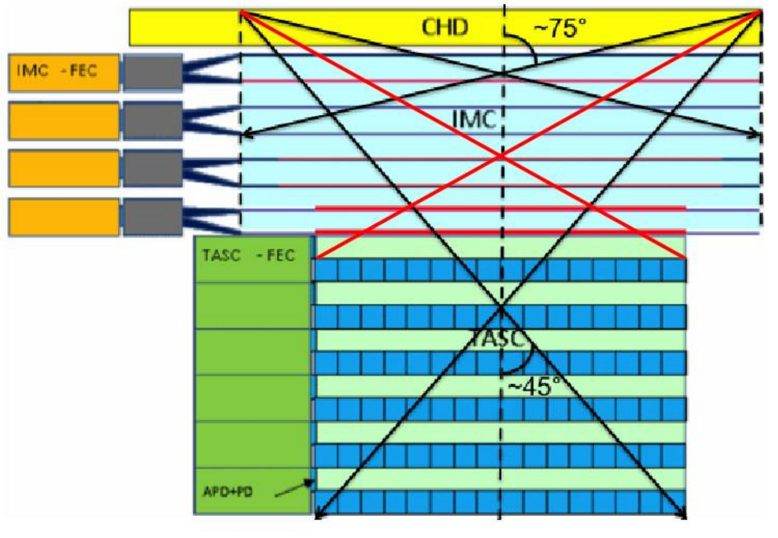

Event Cuts

- For consistency the following events are cut from the analysis
  - Events with a deposited energy less than ~3.7 GeV. Bins below that energy were smeared and prevented a reliable peak fitting from being performed.
  - A instrument cut that accounts for the lack of statistics in the edge cases of the individual paddles, interactions with objects in the FOV, and times where ISS orientation is not standard
  - A consistency cut that requires CHDX and CHDY to be within a 4% percent difference.
  - A minimum deposited energy in the the TASC based on 0.2 GeV/Z.

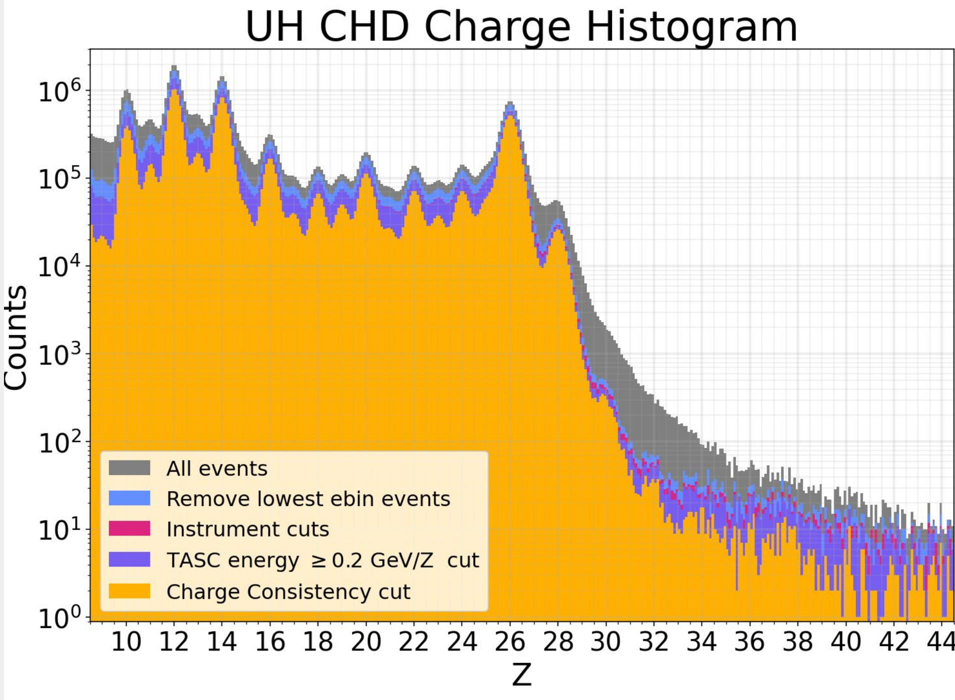

Determination of Abundances

Peak fitting is done over multiple steps.

- Fit step one has minimal constraints to determine sigmas for each peak.
- The sigmas from the even peaks over $8 \leq Z \leq 28$ are then linearly fit to extrapolate a sigma for all peaks
- Second multi-gaussian uses that linearized sigma equation with a maximum-likelihood multiple-Gaussian fit for all elements in CALET's charge range.
- Final fit uses a fixed position and sigma from the second fit to determine error bars on the abundances.

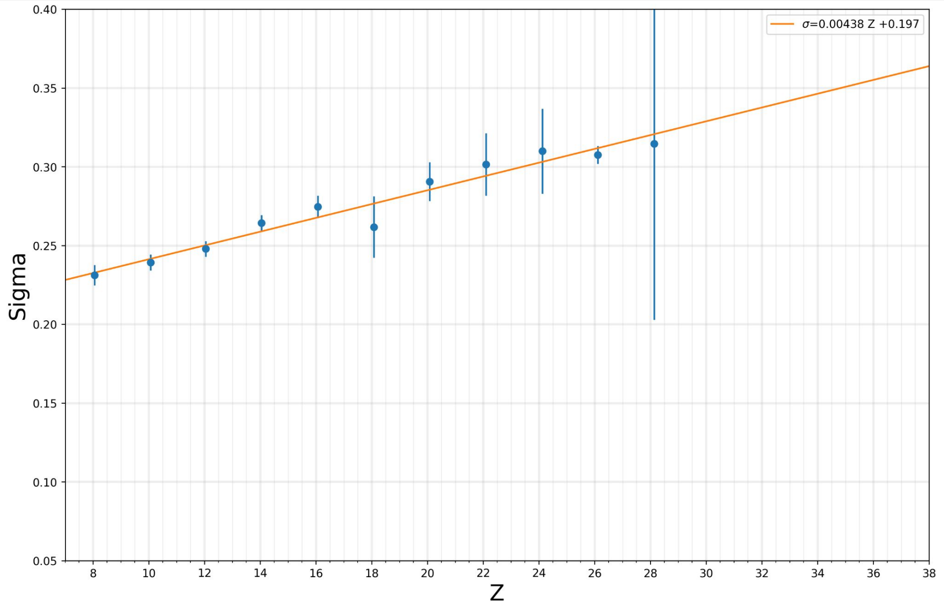

UH TASC CHD charge histogram

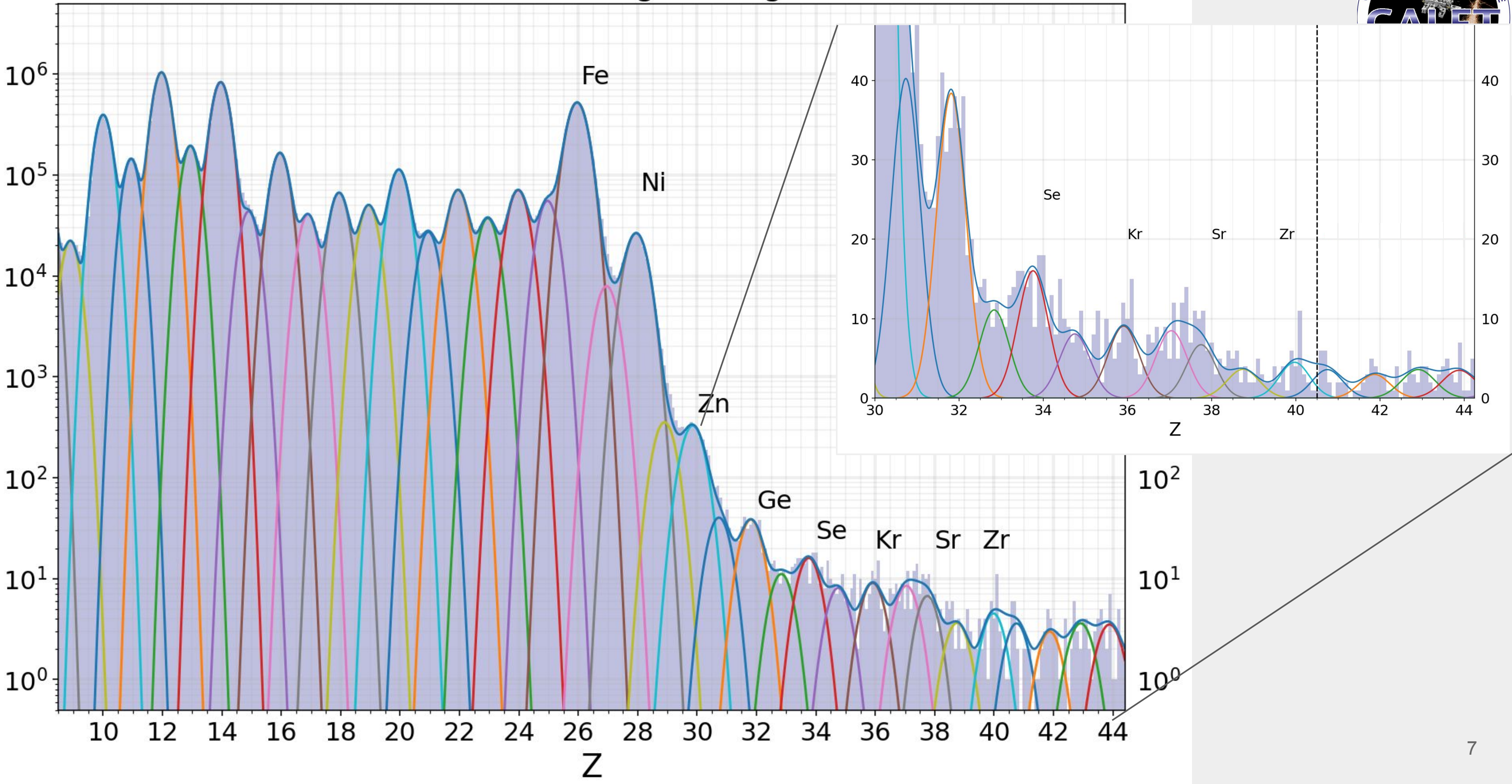

Determining abundances: Simulation vs Experimental

To correct for species- and energy-dependent losses resulting from the analysis cuts, we determine efficiencies with simulated events to match the UH abundances.

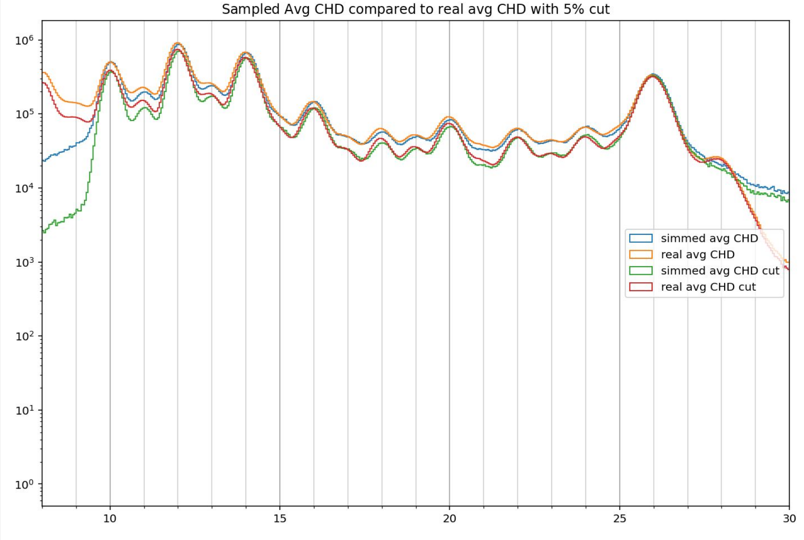

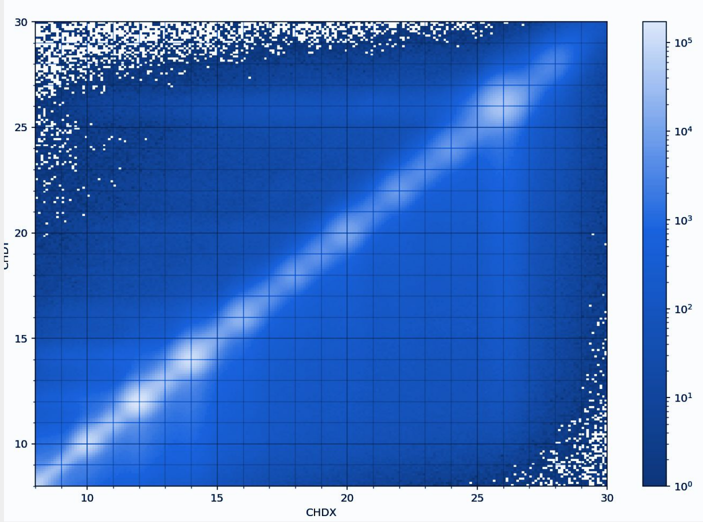

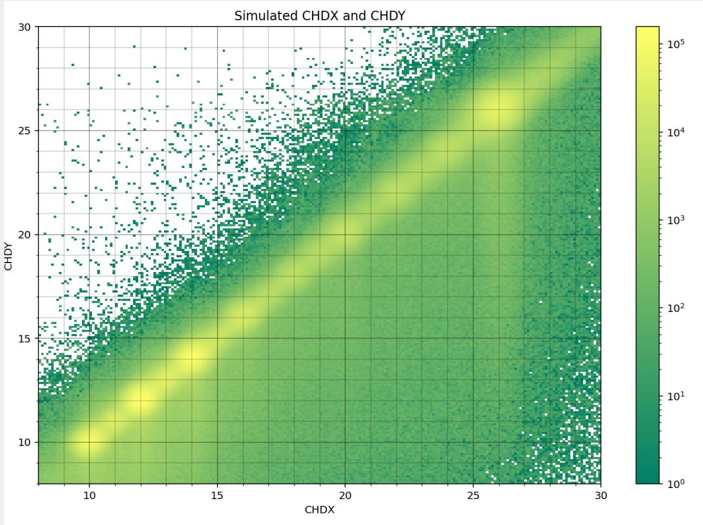

Determining abundances: Correcting for Analysis Systematics

To correct for species- and energy-dependent losses resulting from the analysis cuts, we determine efficiencies with simulated events for Z=10 through Z=39 and from 1 GeV to 550 GeV.

We apply identical cuts as in the analysis and determine a correction factor by finding the ratio of the integral of the corresponding flux over the energy range of interest (right) to the integral of the flux multiplied by the efficiency.

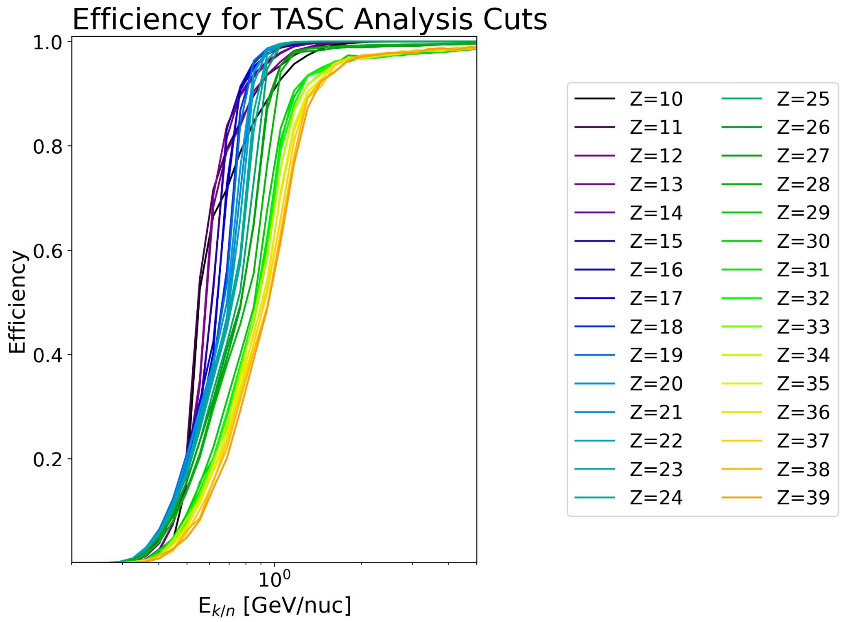

Determining abundances: Correcting for Geomagnetic Screening

As CALET operates within the geomagnetic field, we have to create a time-dependant correction factor for effects of rigidity on nuclei.

Using the approximate energy per nucleon to be detected in this analysis (Simulated 50% efficiency) and convert it to units of magnetic rigidity.

The fraction of time above this geomagnetic rigidity is calculated for each Z using the vertical cutoff rigidity. These values are then normalized to the on-orbit time for $_{26}$Fe and used as a multiplicative factor.

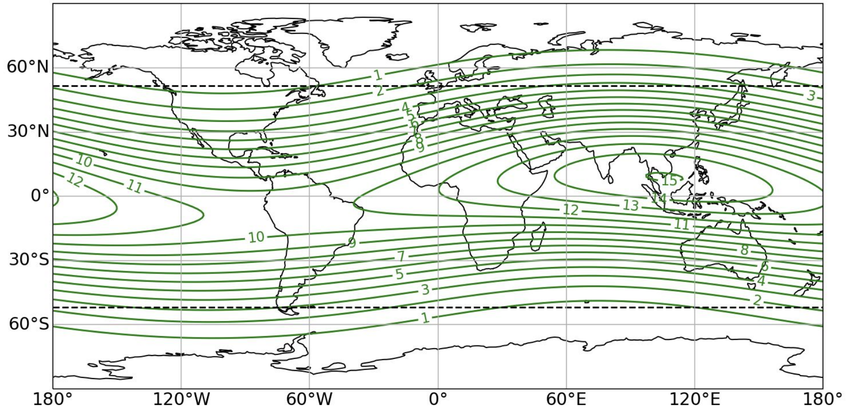

Determining Errors on abundances:

We have three error sources:

- Error from the fitting error. This is calculated from the correlation matrix.
- Gehrels's treatment of poissonian statistical error.
- A systematic error based on the varying the cuts in the analysis to explore how much variance is driven by our choices..

These errors are then combined in quadrature.

An additional multiplicative correction factor is created for the accuracy of cross sections in the simulations where we compare the survival fractions of simulated particles in EPICS to:

1) An analytical model that looks at the interaction mean free paths for each Element and each layer of material traversed through by the particle
2) Additional simulations done in other simulations packages (Geant4) from 10 to 20 GeV/nuc.

Cross Sections

Using total charge changing cross sections from Nilsen (1995):

$$\sigma(R_P,R_T)=\pi[R_P+R_T(3.20\pm0.05)]^2$$

We can calculate the mean free path for each layer:

$$\lambda(P,T) = 1.6624*\left(\frac{\Sigma_T n_T A_T}{\Sigma_T n_T \sigma_{tot}(P,T)}\right)$$

This is then used with the average amount of material passed through for that layer to create the corrective factor:

$$N_{TOI}(Z)=N_{INS}(Z)\prod_i \exp\left[\frac{x_i\langle \sec\theta_{Fe}\rangle}{\lambda_i(Z)}\right]$$

Cross Sections- Differences in models

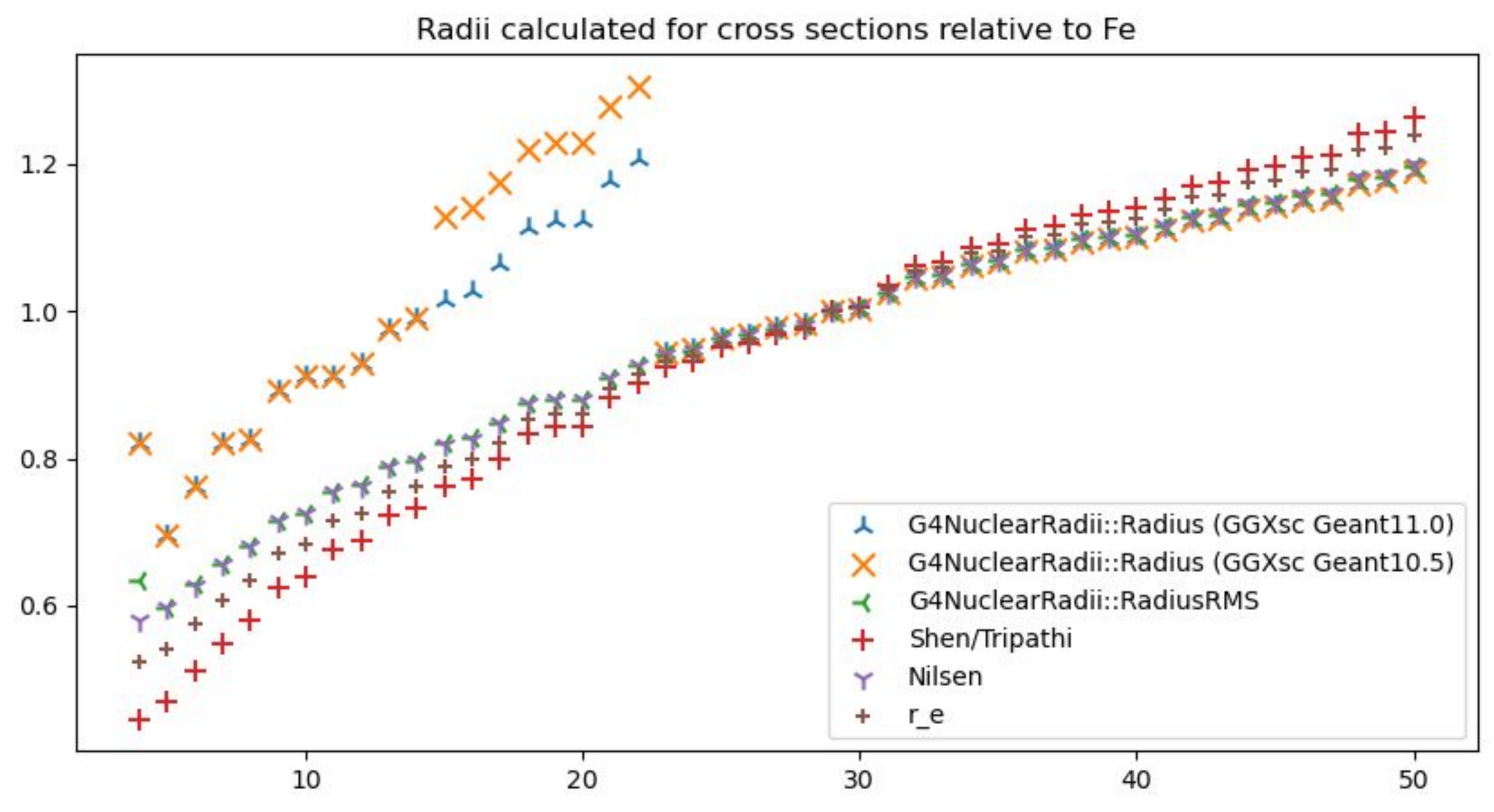

Correction Factors

EPICS uses the DPMJET packages.

Geant4 simulations do not use the default Nuclear radii function as the default function is a piecewise function that has a large discrepancy at A>50.

As such we use two different radii in Geant4. The RMS function and one that produces similar results to EPICS.

For the correction on the analysis we use the EPICS DPMJET simulation and our error bars are adjusted by the maximum and minimum correction factors for each Z.

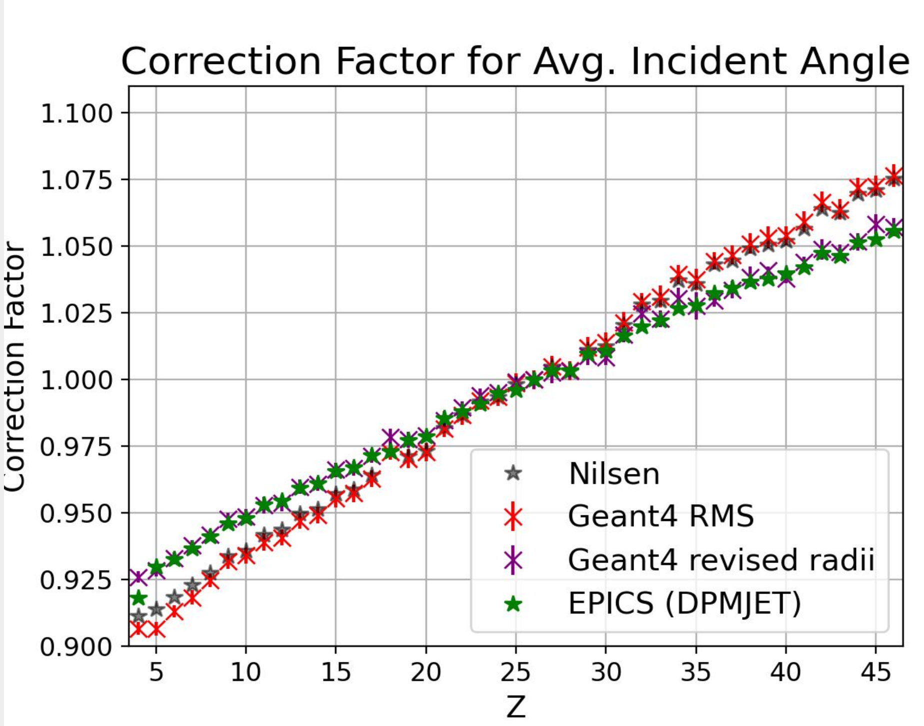

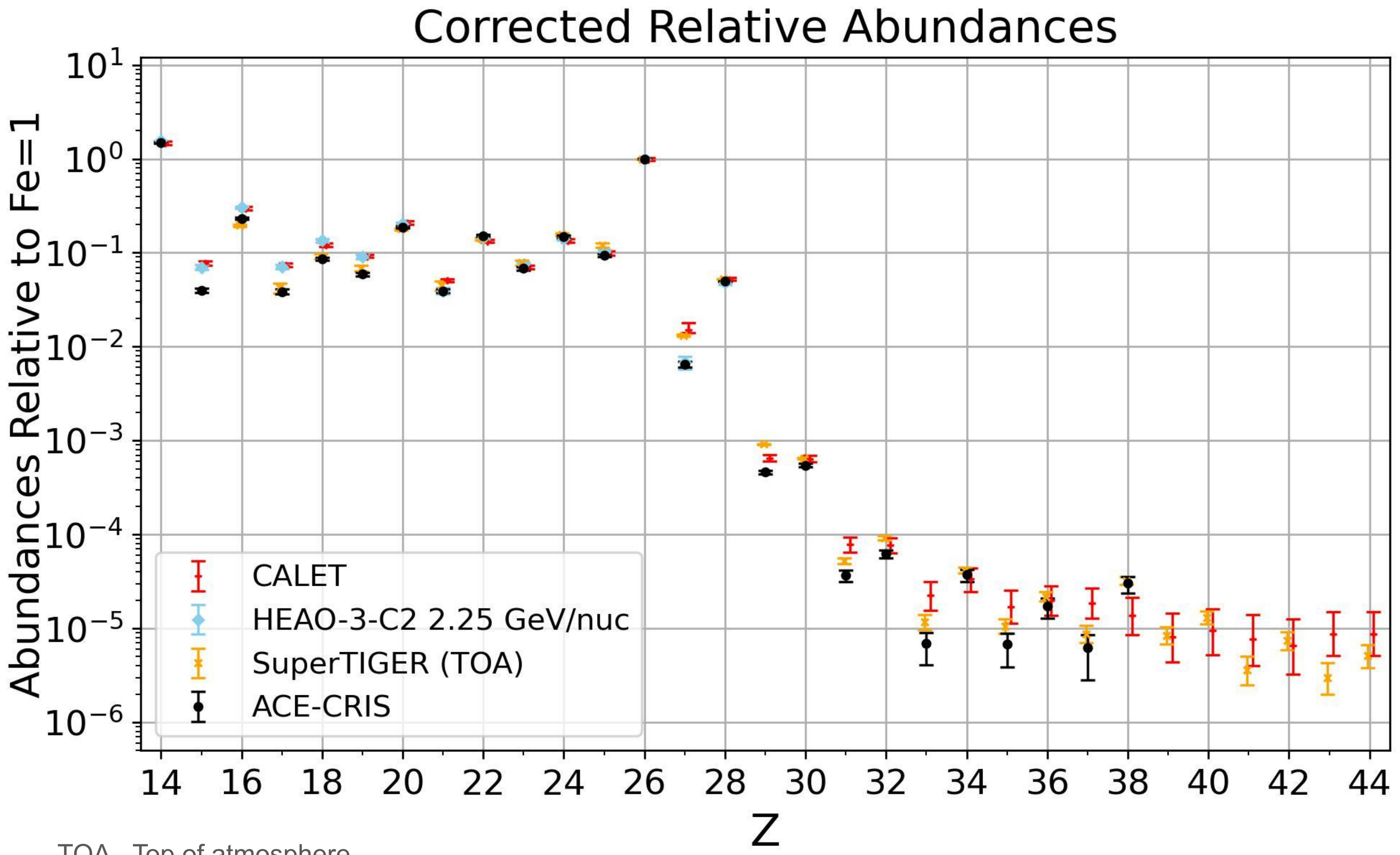

TOA - Top of atmosphere

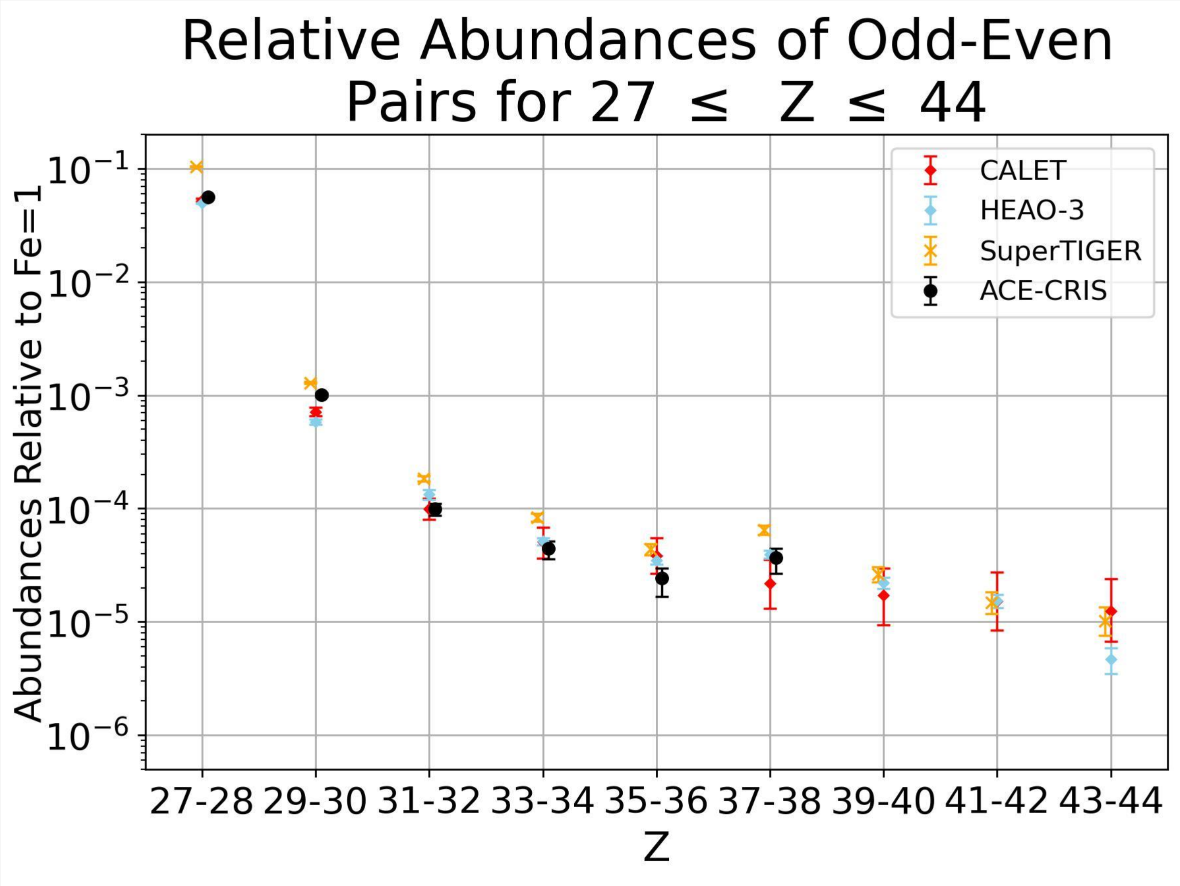
Relative Abundances of Odd-Even
Pairs for 27 ≤ Z ≤ 44
Abundances Relative to Fe=1
10^{-1}
10^{-2}
10^{-3}
10^{-4}
10^{-5}
10^{-6}
27-28 29-30 31-32 33-34 35-36 37-38 39-40 41-42 43-44
Z
CALET
HEAO-3
SuperTIGER
ACE-CRIS

Summary

- The paper for the relative abundances of $14 \leq Z \leq 44$ has been accepted for publication
  - We show consistent results with other published results through Iron.
  - While our higher Z elements have reduced resolution for individual element identification, the odd-even pairs of $Z>26$ are consistent with other measurements from SuperTIGER, HEAO, and ACE-CRIS in our energy range.
- CALET will continue to operating through 2030.

Acknowledgements:

The material is based upon work supported by NASA under award Nos NNX16AC02G and 80NSSC20K0399.

The material contained in this document is based upon work supported by a National Aeronautics and Space Administration (NASA) grant or cooperative agreement. Any opinions, findings, conclusions or recommendations expressed in this material are those of the author and do not necessarily reflect the views of NASA.

Backup Slides

CHD Energy Binned Charge Assignment

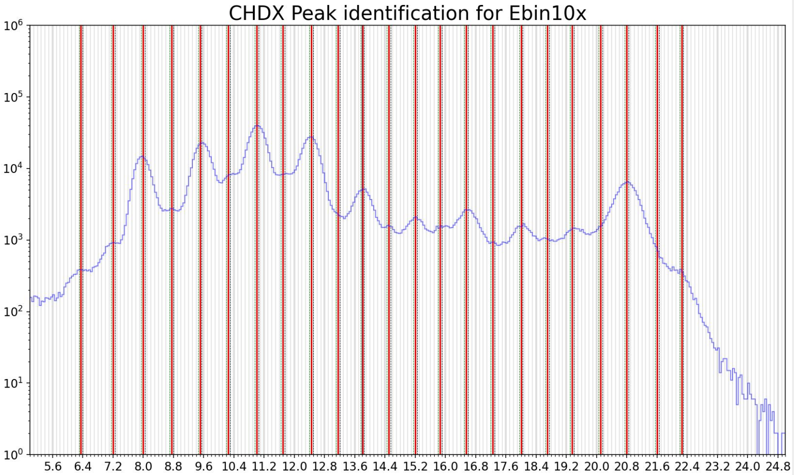

As an example, this the tenth energy bin.
We identify mean peak signal for CHDX (top left) and CHDY.
Plot those peak positions with their respective Z and perform a Tarle Model fit (Bottom Left)
That equation is then used to convert all events within that bin to Z. (Right)

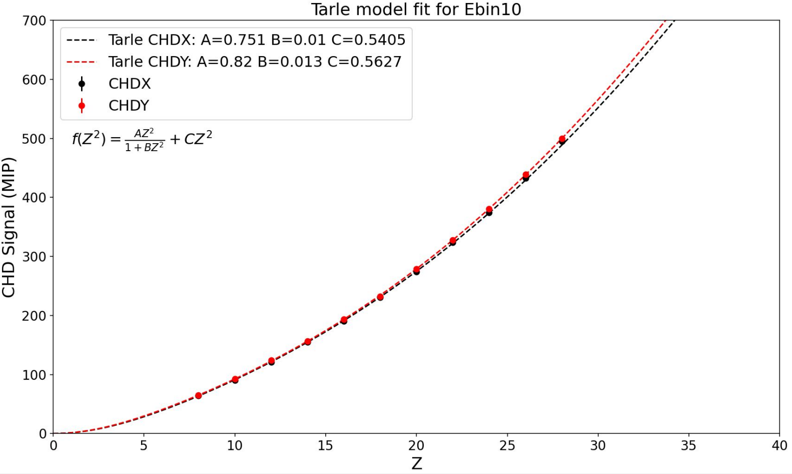

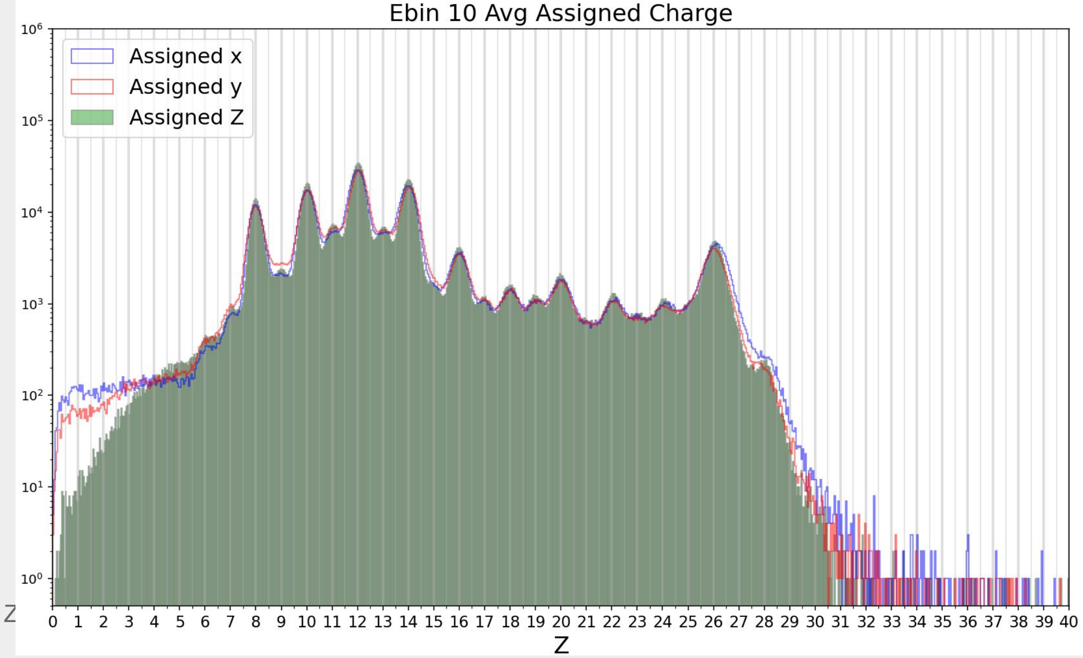

Charge Smearing

Charge smearing at lower energy is shown on top
Lower plot shows a higher energy bin.

Red lines show peak fitting routine's attempt at finding peak position for Tarle charge assignment.

Very noticeable differences in resolving peaks.

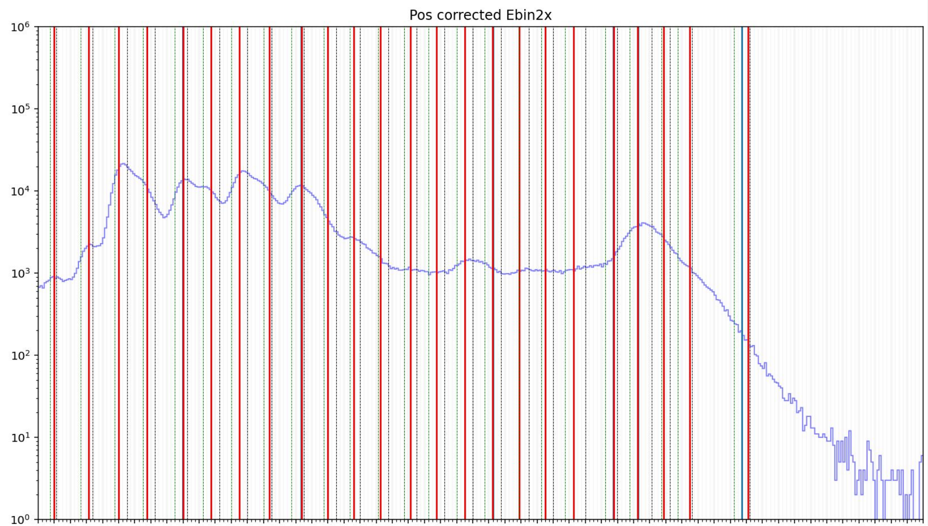

Determination of Variational Error

reuse the fixed parameters from the second fit (sigma and peak position) on a set of alternative histograms. The only thing allowed to vary is peak amplitude.

Error is determined by looking at the maximum and minimum of each abundance relative to Iron.